

Phasic Alertness Impairs Cognitive Control by Amplifying Competition between Evidence Accumulators

 **Jeshua Tromp, Franz Wurm, Federica Lucchi, Roy de Kleijn, and  Sander Nieuwenhuis**

Institute of Psychology, Leiden University, Leiden 2333 AK, The Netherlands

Although phasic alertness generally benefits cognitive performance, it often increases the impact of distracting information, resulting in impaired decision-making and cognitive control. However, it is unclear why phasic alertness has these negative effects. Here, we present a novel, biologically informed account, according to which phasic alertness generates a transient, evidence-independent input (TEI) to the decision process. This shortens overall response times but also amplifies competition between evidence accumulators, thus slowing down decision-making and impairing cognitive control. The key hypotheses of this account are supported with pupil measurements and electrophysiological data from human decision-makers of either sex performing an arrow flanker task. We also show that a computational model of the flanker task that incorporates a TEI can reproduce the behavioral effects of phasic alertness but only when the evidence accumulators compete with each other through lateral inhibition. Our results reveal a close interplay between dynamic changes in alertness, cognitive control, and evidence accumulation.

Key words: arousal; cognitive control; modeling; neuromodulation; oscillations; urgency

Significance Statement

The human attention system is thought to consist of three fundamental components, alerting, orienting, and cognitive control, which shields goal-directed mental activity from distracting information. Although these attentional components are thought to be subserved by distinct brain systems, they seemingly work in concert to produce complicated patterns of behavior. Here, we focus on an interaction between alertness and cognitive control that has puzzled cognitive psychologists for two decades: although increased alertness generally benefits cognitive performance, it disrupts cognitive control. We propose a neurobiologically plausible mechanistic account of how alertness impairs control and support this account with pupil and EEG measurements, as well as computational simulations.

Introduction

The alerting system, one of the attention systems of the human brain, helps us rapidly respond to abrupt environmental changes (Posner, 2008; Petersen and Posner, 2012). Auditory and visual alerting cues that directly precede a target stimulus often benefit performance by enhancing perception (Jepma et al., 2009; Kusnir et al., 2011; Petersen et al., 2017), boosting visual search (Jankovic et al., 2022; Dietze and Poth, 2024) or speeding responses (Posner et al., 1973; Hackley, 2009), even when they provide no information about the correct response. These effects are commonly

attributed to phasic alertness, a transient arousal increase that enhances readiness to respond.

Although the effects of phasic alertness on cognitive performance are generally beneficial, a marked exception is their detrimental effect on cognitive control. These effects occur in decision-making tasks in which individuals must ignore salient but misleading aspects of a stimulus in favor of less prominent but task-relevant information. In these tasks, phasic alertness increases the interference caused by the distracting stimulus elements, even though overall decisions are made more quickly. This counterintuitive pattern of results has been reported in numerous studies in recent decades (Fan et al., 2002; Callejas et al., 2005; Macleod et al., 2010; Böckler et al., 2011; Klein and Ivanoff, 2011; McConnell and Shore, 2011; Fischer et al., 2012; Weinbach and Henik, 2012; Schneider, 2018a, 2020; Kahan and Zhang, 2019). However, it remains unclear why alerting cues impair cognitive control in these contexts: previous theoretical attempts to explain the relevant observations (Callejas et al., 2005; Weinbach and Henik, 2012; Nieuwenhuis and de Kleijn, 2013; Schneider, 2018b) have met with conflicting findings (Schneider, 2018a,b, 2019a,b; Seibold, 2018), and little is known

Received Aug. 22, 2024; revised July 3, 2025; accepted Aug. 21, 2025.

Author contributions: J.T. and S.N. designed research; J.T. and F.L. performed research; J.T., F.W., R.D.K., and S.N. analyzed data; J.T. and S.N. wrote the paper.

J.T. and S.N. were supported by the Netherlands Organization for Scientific Research (Grant Number VIDI.181.032). We thank Peter Murphy for his helpful comments on an earlier draft of the manuscript.

The authors declare no competing financial interests.

Correspondence should be addressed to Jeshua Tromp at jeshuatromp@live.nl.

This paper contains supplemental material available at: <https://doi.org/10.1523/JNEUROSCI.1595-24.2025>

Copyright © 2025 the authors

about the neuroscientific basis of the interaction between alerting and cognitive control.

Here we present a novel, biologically informed account of how phasic alertness impacts decision-making and cognitive control (Fig. 1). The account consists of three key hypotheses, which we support with empirical evidence and computational modeling. First, we hypothesized that alerting cues would cause a transient increase in phasic arousal (Tona et al., 2016), driven by neuromodulatory nuclei of the ascending arousal system (Grant et al., 1988; Joshi et al., 2016). We tested this hypothesis by measuring the effect of auditory alerting cues on the pupil dilation response (PDR), a well-validated correlate of phasic neuromodulatory activity (de Gee et al., 2017; Joshi and Gold, 2020).

Second, we hypothesized that the phasic arousal response to alerting stimuli would produce a transient, evidence-independent neural signal that expedites the evolving decision process by driving evidence accumulators closer to a fixed decision threshold. This hypothesis was inspired by findings suggesting that phasic arousal can generate decision urgency, a monotonically increasing, evidence-independent input to the decision process that human subjects can invoke to speed up their decisions under time pressure (Murphy et al., 2016; Carland et al., 2019). To examine this hypothesis, we assessed the effects of alerting cues and phasic, pupil-linked arousal on an EEG signature of transient, evidence-independent input (TEI) to the decision process.

Third, we hypothesized that TEI to the decision process would increase response conflict. By driving accumulators closer to a fixed decision threshold, TEI signals should speed up decisions. However, if the accumulators representing potential decision outcomes compete with each other through lateral inhibition (Usher and McClelland, 2001), then TEI might also exacerbate the interference from distracting information, thus increasing response conflict and impairing cognitive control. We tested this hypothesis by examining the effects of alerting cues and TEI on behavioral and neural manifestations of response conflict.

The behavioral, pupillometric, and electrophysiological findings reported below provide strong, convergent evidence for our account of how phasic alertness impacts decision-making and cognitive control. We also show that a drift diffusion model (DDM) of the flanker task with incorporated TEI can reproduce the behavioral effects of alerting, but only when the evidence accumulators compete via lateral inhibition.

Materials and Methods

Participants. Sixty-four individuals (41 females), aged between 18 and 28 years, participated in the study in return for a monetary compensation of €14.25. They provided written informed consent, and the study was approved by the Psychology Research Ethics Committee of Leiden University (CEP code, S.T.-V3-2300). Four participants were excluded because they had an error rate of 25% or higher for one of the four trial types (see below), leaving 60 participants for further analyses.

Task design. Participants performed an arrow flanker task, in which the central arrow was flanked by two arrows on either side (Fig. 2a). The

four flanking arrows pointed either in the same direction as the central target arrow (congruent trials) or in the opposite direction (incongruent trials). Each flanker stimulus remained visible for 1,000 ms, irrespective of the participant's response speed. We fixed the stimulus-viewing time to prevent a relationship between response time (RT) and the timing of visually evoked pupil size changes. In half of the trials, an alerting tone (150 ms, 800 Hz, 77 dB) was played 500 ms before the stimulus (alert trials); in the other half, there was no tone (no-alert trials). To minimize previous-trial effects on the pupil size, we let the intertrial interval (ITI) vary randomly between 2,000 and 4,000 ms.

The four trial types (congruent/alert, congruent/no-alert, incongruent/alert, and incongruent/no-alert) occurred equally often and were presented randomly. For each participant, there were 10 blocks with 72 trials each. Eight were catch trials, in which an alerting tone was presented but no flanker stimulus. These catch trials were included to lower the temporal contingency between the alerting cue and the flanker stimulus and thus discourage active temporal preparation during the cue-target interval (see Discussion).

Procedure. We instructed participants to respond quickly and accurately to the direction of the central target arrow. Those who achieved an average RT of 400 ms or faster, with at least 95% accuracy, received an additional €4 compensation. Using a QWERTY keyboard, participants responded by pressing the "A" key with their left index finger for left-pointing arrows and the numeric pad's "6" key with their right index finger for right-pointing arrows. We informed participants about the alerting cues but stressed that these were irrelevant to the task. Furthermore, we instructed participants to fixate their gaze on the central fixation cross presented between flanker stimuli.

Before the main experiment, participants completed a practice block of 16 trials and received feedback on their performance. Participants who did not achieve a 90% accuracy rate repeated the practice block until they did reach that accuracy. Participants were shown their average accuracy and RT after each block in the main experiment.

Pupillometry. To minimize luminance-related pupil-size changes, we presented stimuli and background using isoluminant Teufel colors. The task featured a slate-blue background (RGB 166, 160, 198), salmon-colored arrows, and a salmon-colored central fixation cross (RGB 217, 152, 158). Using a Tobii-Pro eye tracker, we recorded pupil diameter under ambient light below 7.2 cd/m^2 at a 40 Hz sampling rate. Before the main experiment began, we calibrated the eye tracker. During the calibration and the main experiment, participants rested their heads on a chin rest placed 75 cm from the screen.

Due to recording issues with the eye tracker at the start of data collection, we removed the first 29 participants from the pupillometry analysis. Pupil data from the remaining 31 participants were preprocessed using the *gazer* package in R. First, we identified eyeblinks, which resulted in missing data during the blink and unreliable data shortly before and after the blink. For this reason, we also marked the 50 ms before and after the blink as missing data (Mathôt and Vilotjević, 2022). The missing data were filled using linear interpolation, and the resulting data were smoothed with a moving-average filter with a width of 10 samples. All trials with over 50% missing samples were discarded, which amounted to 5.7% of the trials. An analysis of the occurrence and timing of eyeblinks revealed that participants tended to blink after the offset of the flanker stimulus and that there was essentially no difference between experimental conditions (e.g., alert vs no-alert) in the proportion of blinks. Artifacts were identified based on the *max_pupil_dilation* function of the *gazer* package, which implements the outlier detection



Figure 1. Hypothesized causal pathway (and operationalizations, in blue text) explaining the deleterious effect of phasic alertness on cognitive control. Black arrows depict the three key hypotheses.

formula described by Kret and Shak-Shie (Kret and Shak-Shie, 2019). This led to the exclusion of an additional 0.4% of the trials. Lastly, we removed trials where the baseline pupil size deviated from the mean by more than three standard deviations (Mathôt and Vilotjević, 2022), which led to the removal of 4.2% of the trials.

For the timepoint mixed-model regression analyses, we used a sliding window with a length of 100 ms to quantify the effect of trial type on the development of pupil size after the presentation of the alerting stimulus. These pupil time series were *z*-scored before they were entered into a mixed-model regression analysis—one for each window—with the pupil size as the dependent variable, alerting and congruency as independent variables and subject as a random intercept to account for between-subject variability. Informed by these analyses, we took the mean baseline-corrected pupil size in the interval between 0 and 200 ms after the flanker stimulus onset as our PDR measure for the trial-wise mixed-model analyses. During this interval, the pupil size showed a significant effect of alerting but not congruency. To baseline-correct the data, we used the interval from 600 to 500 ms before the stimulus onset (i.e., the 100 ms before the potential presentation of the alerting stimulus).

Importantly, we found substantial time-on-task effects on the PDR within blocks but not over the whole experiment. Because the PDR was substantially larger at the start of each block, we excluded the first five trials of each block before fitting the trial-wise mixed models described below.

EEG data collection and preprocessing. Continuous EEG data were acquired using an ActiveTwo system (<http://biosemi.com>) from 64 scalp electrodes, configured to the standard 10/20 setup, and digitized at 512 Hz. Eye movements were recorded using two electrodes positioned above and below the left eye and two electrodes positioned at the outer canthus of each eye. Electrodes placed on the mastoids served as reference points.

We preprocessed the EEG data of 60 participants using a combination of manual and automatic preprocessing steps using the Python package MNE. First, we checked for electrode bridging. If bridging was present, we interpolated these electrodes. Next, we low-pass filtered the data at 0.5 Hz and cut the data into epochs around the stimulus onset (−3,500–2,000 ms) and around the response (−3,500–2,000 ms). These wide time ranges prevented edge artifacts in the time-frequency decomposition described below. We then utilized an automated algorithm for unified rejection and repair of bad epochs called *autoreject*. First, we identified bad epochs using a first-pass *autoreject*, after which we conducted an ICA (using the Picard method) to filter out these bad epochs. This filter significantly increased the quality of the ICA components. After manual component rejection (mainly focused on eyeblink artifacts and other artifacts in the signal that we could clearly distinguish from brain activity), we re-ran the *autoreject* algorithm over all epochs, including trials excluded from the ICA. Finally, we visually inspected the EEG data. If key electrodes were still noisy or the *autoreject* algorithm rejected >30% of the epochs, we removed the participant from the analysis. This exclusion criterion led to removing 7 of the 60 analyzed participants. Four additional participants were excluded from the midfrontal time-frequency analysis because of faulty/bridged frontal electrodes. A summary of each step of the preprocessing pipeline can be reviewed for each participant in the *osf* data storage (<https://osf.io/an4sv/>).

EEG surface Laplacians over the motor areas. Next, we estimated the surface Laplacian (current source density) for response-locked epochs using a 10th-order Legendre polynomial. We set the regularization parameter (λ) to 10^5 to optimize the balance between data representation fidelity and the smoothness of the estimated current source densities. This method accentuates local neural activities while minimizing the impact of volume conduction, thus enhancing the spatial resolution of the EEG data.

For the surface Laplacian analysis, we took the response-locked epochs and baselined these epochs by subtracting the mean of the baseline period 1,700–1,500 ms before the response from the entire signal. This time window ensured the baseline period was in the ITI, regardless of response speed. We redefined the signals of the C3 and C4 electrodes

as ipsilateral and contralateral motor cortex signals, depending on which response was required. After visually inspecting the condition-average ipsilateral and contralateral waveforms, we identified the time window from −300 to −200 ms before the response as a suitable single-trial measure (see trial-wise mixed models below) for investigating TEI modulations of decision-related ipsilateral and contralateral motor cortex activity. An earlier time window (e.g., 400–300 ms before the button press) would not have captured the TEI modulation on trials with relatively fast RTs (~300 ms).

Note that in previous EEG work, we studied preparatory motor activity by examining oscillatory power in the mu (8–14 Hz) frequency range (Murphy et al., 2016). However, in the current study, RTs were so fast that motor-related mu signals were contaminated by the influence of the stereotyped global decrease in 8–14 Hz power that tends to occur immediately after the stimulus onset.

EEG time-frequency analysis. For all time-frequency analyses, we decomposed the EEG time series into their time-frequency representations by convolving them with a set of Morlet wavelets and applying a fast Fourier transform to both the wavelets and the EEG data. The width of the Gaussian of the Morlet waves was set based on frequency: two cycles for frequencies <2 Hz, four cycles for frequencies <3 Hz, and six cycles for higher frequencies. These cycles yielded a good trade-off between temporal and frequency resolution.

For the response-locked time-frequency scalp plots (Fig. 6), we narrowed the frequency range to 4–8 Hz (i.e., theta) and split this range into 10 log-spaced bins. We then applied a log-ratio baseline correction using a baseline period of 1,700–1,500 ms before the response, resulting in decibel-normalized power (decibel). Next, we plotted the scalp topographies around the response (−150, 0, and 150 ms) and identified the midfrontal electrodes (FCz and Cz) as the locus of increased theta power, in line with previous findings (van Driel et al., 2015). Then, we ran a new time-frequency decomposition over the midfrontal electrodes with a broader frequency range. We increased the frequency from 1 to 40 Hz in 40 logarithmically spaced steps, with a subsequent log-ratio baseline correction. This time-frequency decomposition with a broad frequency range allowed us to test whether the conflict effect in the midfrontal electrodes was specific to the theta band. For the trial-wise mixed-model analyses that include theta power, we selected the time window from −200 to 100 ms around the response (cf. van Driel et al., 2015). We calculated the mean decibel for that time window for all frequencies between 4 and 8 Hz.

Experimental design and statistical analyses. We conducted the single-trial statistical analyses in RStudio using the lme4 package for building and fitting linear mixed models. For all mixed-model analyses, we filtered out the incorrect trials (except for Eq. 1b). As independent variables, we took the mean of contralateral and ipsilateral motor activity (mean contra/ipsi), the difference between contralateral and ipsilateral motor activity (diff contra-ipsi), and response-locked theta power (theta), *z*-scored separately for each participant, as well as the sizes of the “PDR” and baseline pupil (BP), *z*-scored separately for each participant and block. As dependent variables, we took RT, mean contra/ipsi, diff contra-ipsi, and theta. These dependent variables were *z*-scored over all participants because the mixed models already took into account between-subject differences in the dependent variables; each model included a random intercept for each participant. To highlight the important results of these mixed models, we visualized them by dividing the independent variable into 10 equally populated bins and showing the correlation with the dependent variable. Note, however, that the statistical tests were based on single-trial data, not binned averages. All mixed models are described using the R notation style.

First, we ran the following mixed model:

$$\text{RT} \sim \text{alert} * \text{cong} + (1|\text{subject}), \quad (1a)$$

where alert denotes whether an alerting cue preceded the trial and cong denotes whether the trial was congruent. The interaction term allowed us to test the key hypothesis that the congruency effect on RT (partly) depends on the alerting cue.

Second, we ran the following model:

$$\text{accuracy} \sim \text{alert} * \text{cong} + (1|\text{subject}), \quad (1b)$$

where accuracy is a binary variable denoting whether the response on a trial was correct. As the accuracy variable is binary, we ran a mixed model with a binomial distribution (in all the other models, we used the standard Gaussian distribution).

Next, we investigated pupil-related measures as follows:

$$\text{RT} \sim \text{alert} * \text{cong} + \text{cong} * \text{PDR} * \text{BP} + (1|\text{subject}). \quad (2)$$

Followed by mixed models investigating the mean contra/ipsi measure as follows:

$$\text{mean contra/ipsi} \sim \text{alert} * \text{cong} + (1|\text{subject}), \quad (3)$$

$$\text{diff contra-ipsi} \sim \text{alert} * \text{cong} + (1|\text{subject}). \quad (4)$$

We predicted that alert trials would be characterized by a bilateral, not unilateral, increase in motor cortex activity. If that is the case, mean contra/ipsi should show an association with the alerting cue, but diff contra-ipsi should not.

To test our prediction that the bilateral increase in motor cortex activity depends on the size of the PDR, we ran the following mixed model:

$$\text{mean contra/ipsi} \sim \text{PDR} + \text{BP} + \text{alert} * \text{cong} + (1|\text{subject}). \quad (5)$$

Next, we tested whether we could predict RT from mean contra/ipsi as follows:

$$\text{RT} \sim \text{alert} * \text{cong} * \text{mean contra/ipsi} + (1|\text{subject}). \quad (6)$$

Then, we tested whether theta power at the time of the response was modulated by congruency, the alerting cue, and their interaction as follows:

$$\text{theta} \sim \text{alert} * \text{cong} + (1|\text{subject}). \quad (7)$$

Subsequently, we tested the relationship between theta power and mean contra/ipsi versus diff contra-ipsi, with the prediction that theta should depend on the former but not the latter as follows:

$$\text{theta} \sim \text{mean contra/ipsi} + \text{alert} * \text{cong} + (1|\text{subject}), \quad (8)$$

$$\text{theta} \sim \text{diff contra-ipsi} + \text{alert} * \text{cong} + (1|\text{subject}). \quad (9)$$

Lastly, we ran causal mixed-model mediation analyses (Tingley et al., 2014) to assess whether PDR and mean contra/ipsi mediated the effects of the alerting cue on RT. Our analysis plan was not preregistered.

Computational modeling. We conducted model simulations to test whether a TEI to the decision process can explain the well-established effects of alerting on overall response speed and the flanker congruency effect. As the basis for our simulations, we took a previously successful sequential-sampling model of the flanker task as a starting point: the shrinking spotlight (SSP) model (White et al., 2011; Weichart et al., 2020). The SSP model is a variant of the standard DDM for two-alternate decisions. The standard DDM model assumes that one accumulator accumulates noisy sensory input from a starting point z at a drift rate v . A decision is made when the accumulator reaches decision threshold a or $-a$ (representing the two choices). All nondecision-related processing is captured in the nondecision time parameter t_{er} .

The difference between the standard DDM and the SSP models we used is twofold. First, the standard DDM assumes a constant drift rate over time, while the SSP models include a time-variant drift rate. The time-variant drift rate in the SSP models is meant to implement the attentional spotlight hypothesis of the flanker congruency effect, which

assumes that attention gradually narrows in on the target during the trial. At the stimulus onset, the spotlight is relatively wide, allowing the flankers to impact evidence accumulation; however, over the trial, attentional selection gradually reduces the spotlight width, leading the target arrow to dominate evidence accumulation. This hypothesis captures the commonly found below-chance drop in accuracy at fast RTs and other aspects of the conditional accuracy function (Gratton et al., 1988). Second, the standard SSP model (White et al., 2011) has “one” accumulator with “two” decision boundaries, whereas the SSP models we used (Weichart et al., 2020) have “two” accumulators that race toward a single (common) decision threshold. These two-accumulator variants allowed us to add a TEI to both accumulators (Murphy et al., 2016).

In the SSP model, the time-variant drift rate is governed by three parameters: perceptual input strength (p), the width of the spotlight at the beginning of the trial (sd_0), and the rate at which the spotlight shrinks (r_d). The spotlight is a density function for a Gaussian distribution centered around 0, with standard deviation sd_a . At each time point, the width of the spotlight is given by the following equation:

$$sd_a = sd_0 - r_d t,$$

with t defining the time point of the trial and sd_a defining the spotlight width at time point t . The resulting area of attention directed toward the target and the flankers is given by the following equation:

$$\begin{aligned} a_{\text{target}} &= \int_{-0.5}^{0.5} \mathcal{N}(0, sd_a) \\ a_{\text{flanker}} &= \int_{0.5}^{n+0.5} \mathcal{N}(0, sd_a), \end{aligned}$$

where n denotes the number of flankers (set to a value of 1) and a denotes the area under the curve. Furthermore, we assume that each arrow (flanker or target) occupies one unit of space. To simulate the effect of a wider spacing between targets and flankers, we moved the flanker 0.25 away from the target so it extended from +0.75 to +1.75.

Finally, the drift rate is given by the following formulas, depending on congruency:

$$\text{congruent: } \rho_c = p a_{\text{target}} + 2p a_{\text{flanker}} ; \rho_{-c} = 0,$$

$$\text{incongruent: } \rho_c = p a_{\text{target}} ; \rho_{-c} = 2p a_{\text{flanker}},$$

where ρ_c denotes the drift rate for accumulator c , ρ_{-c} denotes the drift rate for the

opposing accumulator, and p denotes the perceptual input strength parameter.

We implemented two variations of the SSP model: the feedforward inhibition (FFI) variant and the leaky-competing accumulator (LCA) variant (Weichart et al., 2020). These variants mainly differ in how the two competing accumulators relate. In the FFI variant, the accumulators are perfectly anticorrelated (cf. Murphy et al., 2016). This mimics the dynamics of the single-accumulator (standard) SSP model, where a movement toward one decision threshold necessitates a movement away from the other. The following formula describes the accumulation of evidence in the FFI:

$$\begin{aligned} \text{drive}_c &= \rho_c \frac{dt}{\Delta_t} + \xi_t \sqrt{\frac{dt}{\Delta_t}} \\ \text{dx}_c &= \text{drive}_c - \text{drive}_{-c}, \\ x_c &\rightarrow \max(x_c, 0). \end{aligned}$$

Evidence for accumulator c is denoted x_c (with a lower bound of 0); dx_c denotes the change in evidence on timestep t ; ρ_c denotes the drift rate for accumulator c ; drive_{-c} represents drive for the opposing choice with respect to c , and noise is represented by ξ_t , a driftless Wiener process centered around 0. We used the Euler method to discretize time, selecting a step size of $dt = 0.01$ modified by a time constant of $\Delta_t = 0.1$ —the same values

as in Weichert et al. (2020). Simulated trials on which the incorrect accumulator crossed the decision threshold first were considered error trials.

In the LCA variant, the accumulators are not perfectly anticorrelated, but they inhibit each other to a certain extent through lateral inhibition, as given by parameter β . Additionally, in the LCA variant, the evidence in each accumulator passively decays throughout the decision process at a rate equal to leak parameter κ as follows:

$$dx_c = (\rho_c - \kappa x_c - \beta x_{-c}) \frac{dt}{\Delta t} + \xi \sqrt{\frac{dt}{\Delta t}},$$

$$x_c \rightarrow \max(x_c, 0),$$

For further mathematical details of the SSP-FFI and SSP-LCA models, see Weichert et al. (2020).

The approach we took was as follows. First, we fitted the two models to the empirical behavioral data in the no-alert condition. To determine the best-fitting set of model parameter values, we used a Bayesian optimization algorithm called Bayesian adaptive direct search to minimize a cost function that calculated, for each level of congruency, the difference between the empirical and simulated median RTs, between the empirical and simulated standard deviations (SD), and between empirical and simulated accuracy (Singh and Acerbi, 2024). The resulting differences were normalized by dividing by the empirical median RT, mean SD, and mean accuracy and then summed (Bogacz and Cohen, 2004). We fitted the models to these metrics because they reflect the typical flanker congruency effects and alerting effects reported in the literature. We specified uninformative priors for each parameter (Table 1). For each fitted parameter set, we simulated 10,000 trials per condition.

To assess the predictive accuracy and robustness of the FFI and LCA model fits, we carried out a Monte Carlo cross-validation procedure. We randomly split the dataset of each participant into two equal halves and then averaged across participants. One-half of the data was used for training the full model (including urgency parameters) using the model-fitting procedure described above, and the other half of the data was used for testing. Model performance was quantified as the difference between empirical and simulated data for each of the six metrics mentioned above. This process was repeated 200 times. Table S1 reports the root mean squared error for each of the two models and six metrics. These results suggest that the models had adequate predictive accuracy.

Our next step was to fit the two models to the empirical behavioral data in the alert condition. Therefore, we fixed all SSP parameters to the best-fitting values in the no-alert condition and added two free TEI parameters to simulate the effects of the alerting cue. The TEI signal was a time-variant function with a positive intercept and a negative slope, which was added as an evidence-independent input to both accumulators evenly as follows:

$$\text{TEI} = \text{TEI}_{\text{intercept}} + \text{TEI}_{\text{slope}} * t,$$

$$\text{TEI} \rightarrow \max(\text{TEI}, 0),$$

$$dx_{c-\text{TEI}} = dx_c + \text{TEI},$$

Table 1. Overview of parameters, bounds, and best fits for both FFI and LCA

Parameter	Description	Bounds	Best-fit FFI	Best-fit LCA
r_d	Rate of focus	(0,30)	19.96	4.80
p	Perceptual input strength	(0,20)	1.95	6.24
sd_a	Starting spotlight width	(0,5,5)	1.69	0.72
a	Decision threshold	(0,30)	5.54	12.80
ξ	Noise	(0,1,5)	1.13	3.67
t_{er}	nondcision time	(0,1,0,30)	0.24	0.26
β	Lateral inhibition	(0,1)	–	0.65
κ	Leak	(0,1)	–	0.19
$\text{TEI}_{\text{intercept}}$	TEI intercept	(0,5)	0.06	0.6
$\text{TEI}_{\text{slope}}$	TEI slope	(−10,10)	−1.1	−6.52

The lateral inhibition and leak parameters are absent in the FFI models.

where $dx_{c-\text{TEI}}$ denotes the change in evidence for timestep t , including TEI. The TEI signal was constrained to be positive or zero. The model-fitting procedure was the same as for the no-alert condition. After acquiring the best-fitting TEI parameters for the FFI and LCA model variants, we conducted a grid search with 100,000 simulations per grid around the best-fitting TEI parameter combination to find out how robust the resulting TEI effect (average speed-up) and TEI-congruency effect (average increase in congruency effect due to the TEI) were.

Results

Auditory alerting cues speed up responding and increase flanker congruency effect

Participants ($N=60$) performed 640 trials of an arrow flanker task (Fig. 2a), in which they were to identify the direction of the middle arrow (target) using their left or right index finger, as quickly and accurately as possible. On congruent trials (50%), the four flanker arrows pointed in the same direction as the target arrow; on incongruent trials (50%), they pointed in the opposite direction. In addition, on half of the trials, we presented a brief, uninformative auditory alerting cue starting 500 ms before the stimulus onset. We chose this cue-target interval because it is the most-used interval in alerting-control studies and because it allowed us to distinguish the pupil and EEG responses associated with the alerting cue and flanker stimulus. The mixed-model equations we used to analyze the data are described under Materials and Methods and cited below.

Median correct RTs (Fig. 2b; Table 2) showed the expected effects of alerting, congruency, and their interaction: RTs were slower on incongruent trials than on congruent trials (Eq. 1a, $\beta=-0.57$; 95% CI [−0.59, −0.55]; $t_{(36813)}=-48.60$; $p<0.001$) and faster on alert trials than on no-alert trials ($\beta=-0.18$; 95% CI [−0.20, −0.16]; $t_{(36813)}=-15.26$; $p<0.001$). Importantly, we also replicated the typical alert-congruency interaction effect: the congruency effect was significantly larger on alert compared with no-alert trials ($\beta=-0.20$; 95% CI [−0.23, −0.16]; $t_{(36813)}=-11.87$; $p<0.001$). This effect of alerting on the congruency effect was especially large on trials with a relatively small baseline pupil (Eq. 2, three-way interaction, $\beta=0.03$; 95% CI [0.007, 0.06]; $t_{(16689)}=2.56$; $p<0.05$), which are presumably characterized by relatively low baseline arousal, thus offering more scope for a strong phasic arousal effect (Brown et al., 2015). Furthermore, at the participant level, we found a significant relationship between the magnitude of the alerting effect and the alert-congruency interaction (Fig. 2c; $\beta=0.56$; 95% CI [−0.86, −0.26]; $t_{(58)}=3.73$; $p<0.001$), suggesting that these effects reflect a common underlying process.

As expected, error rates (Fig. 2b; Table 2) were larger on incongruent trials than on congruent trials (Eq. 1b, $\beta=-0.85$; 95% CI [−1.00, −0.70]; $p<0.001$). Overall, alerting did not lead to increases in error rates ($\beta=-0.03$; 95% CI [−0.15, 0.09]; $p=0.60$). Importantly, the congruency effect was increased on alert trials ($\beta=-0.75$; 95% CI [−0.99, −0.51]; $p<0.001$), mirroring the RT findings.

Alerting cues elicit a phasic arousal increase

To assess if alerting cues elicited a phasic arousal increase, we compared the average pupil waveforms obtained in the four task conditions using a sliding-window mixed-model approach with a window length of 100 ms ($N=31$; Fig. 3). A significant alerting effect on the PDR emerged ~400 ms after the alerting cue (and 100 ms before the onset of the flanker stimulus) and

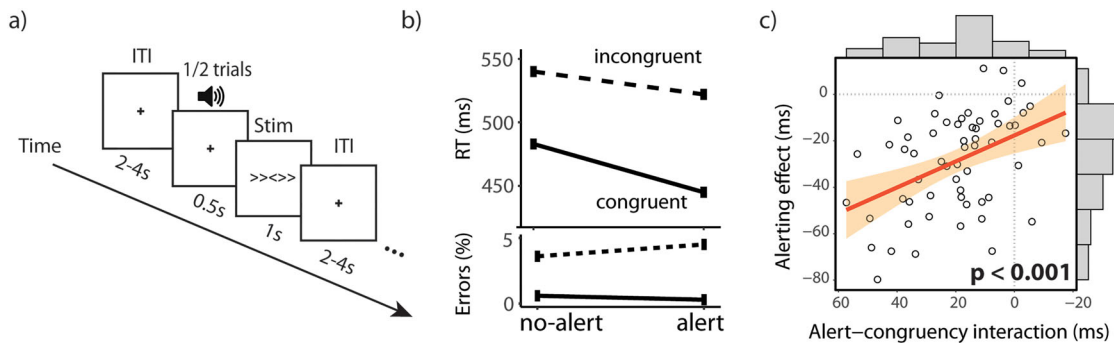


Figure 2. Task and behavioral results. **a**, Example of an incongruent trial in the arrow flanker task. The cue was a 150 ms, 800 Hz, 77 dB tone. **b**, Median RTs and error rates as a function of congruency and alert condition. **c**, A scatterplot of alerting effect and alert–congruity interaction per participant, with distributions on top and right showing the interindividual variability in these effects. The *p* value taken from mixed-model regression described in the main text. ITI, intertrial interval.

Table 2. Median RTs and error rates (SD)

Alert	No-alert	
	Cong	Incong
RT (ms)	428 (83)	507 (95)
Err (%)	1.3 (0.1)	6.1 (0.2)

lasted for 2 s. A significant effect of congruency, consistent with previous studies (van der Wel and van Steenbergen, 2018), emerged much later in the trial, ~900 ms after the onset of the flanker stimulus. We used these waveforms to extract a pupillary single-trial measure of phasic arousal (Tona et al., 2016) for use in subsequent analyses. To rule out any contribution from the pupil response associated with the flanker stimulus, we took the average pupil size in the 200 ms after the onset of this stimulus (Mathot, 2018).

Alerting cues and pupil-linked arousal are associated with an EEG motor preparation signature of TEI

To test the second hypothesis of our theoretical account, we examined if alerting cues and the size of the PDR were associated with TEI to the decision process. As indirect support for this hypothesis, decisions under time pressure, which require a “sustained” evidence-independent input to the decision process (i.e., urgency), are accompanied by larger PDRs (Murphy et al., 2016; Steinemann et al., 2018; Gross and Dobbins, 2021; Poth, 2021) and a modulation of activity in the premotor cortex and primary motor cortex before activity reaches a fixed firing-rate threshold (Thura and Cisek, 2016). As a direct readout of TEI modulations in the motor cortices ipsilateral and contralateral to the correct response hand, we computed the response-locked Laplacian-transformed EEG waveforms at electrodes C3 and C4 (Fig. 4a; $N = 53$; Vidal et al., 2015). These waveforms showed an early activation of the ipsilateral (incorrect) motor cortex, reflecting the transient impact of incongruent flankers. This was followed by a rapid buildup of activity in the contralateral (correct) motor cortex, which typically peaks around the EMG onset (not measured here) and is accompanied by inhibition of the ipsilateral motor cortex (Vidal et al., 2015).

Importantly, on alert trials, the two motor cortices showed a similar-sized cue-evoked TEI modulation, which commenced around the (average) onset time of the flanker stimulus. To quantify the TEI modulations, we took the average amplitude of the EEG waveforms in the interval from 300 to 200 ms before the button press. An earlier time window (e.g., 400–300 ms before

the button press) would not have captured the TEI modulation on trials with relatively fast RTs (~300 ms). A statistical analysis confirmed the additive nature of the TEI modulation (Fig. 4b): the mean of contralateral and ipsilateral motor cortex activity increased after alerting cues (Eq. 3, $\beta = -0.06$; 95% CI [−0.07, −0.04]; $t_{(28609)} = -7.21$; $p < 0.001$), while their difference did not (Eq. 4, $\beta = -0.004$; 95% CI [−0.02, 0.01]; $t_{(28609)} = -0.40$; $p = 0.69$). Furthermore, focusing on participants who had both valid pupil and valid EEG data ($N = 29$), we found that trials with a larger PDR were generally associated with larger mean motor cortex activity (Fig. 4c; Eq. 5, $\beta = -0.01$; 95% CI [−0.02, −0.003]; $t_{(14866)} = -1.15$; $p < 0.01$), demonstrating a direct positive relationship between our measures of phasic arousal and TEI.

EEG signature of TEI predicts speed of responding and flanker congruency effect

Our account of how phasic alertness impacts decision-making and cognitive control assumes that TEI is the cause of both the speed-up of RTs and the increase in the flanker congruency effect, a behavioral manifestation of response conflict. Therefore, our EEG signature of TEI should show this same relationship with RTs. Indeed, we found both a significant main effect of mean contra/ipsi on RT (Eq. 6, $\beta = 0.06$; 95% CI [0.02, 0.09]; $t_{(28605)} = 2.98$; $p < 0.01$) and a significant interaction between mean contra/ipsi and congruency (Fig. 5a; $\beta = 0.08$; 95% CI [0.03, 0.13]; $t_{(28605)} = 3.01$; $p < 0.01$). Because the shape of this important interaction effect is not evident in Figure 5a, we plotted data generated by the best-fitting mixed model in Figure 5b. This figure illustrates that RTs decreased with increasing bilateral motor cortex activity in both congruency conditions but less so in the incongruent condition, suggesting that flanker interference increased with TEI.

Alerting cues and EEG signature of TEI are associated with enhanced midfrontal conflict-related theta-band power

Next, we asked if the apparent increase in response conflict on alert trials (as reflected in greater mean motor activity and increased behavioral congruency effects) was accompanied by an increase in midfrontal theta power, an EEG index of response conflict (Cohen and Cavanagh, 2011; van Driel et al., 2015). In line with previous research, we found an increase in midfrontal theta power around the time of the response (Fig. 6A; $N = 49$). To examine the typical effect of response conflict on midfrontal theta power (Cohen and Cavanagh, 2011; van Driel et al., 2015), we examined the incongruent–congruent difference waveform.

The conflict effect revealed by this difference waveform peaked around the time of the response (Eq. 7; main effect of congruency, $\beta = -0.13$; 95% CI $[-0.16, -0.10]$; $t_{(26759)} = -7.98$; $p < 0.001$) and was specific for the theta frequency range (Fig. 6B). Importantly, the conflict effect was stronger on alert trials than

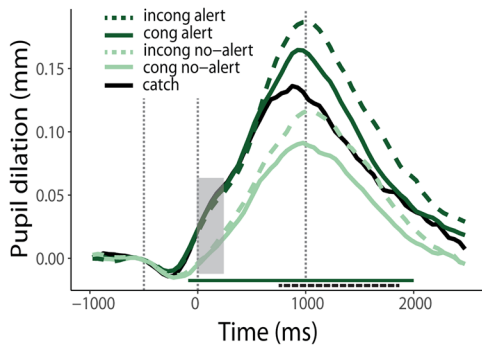


Figure 3. The alerting cue and congruency of the flankers impact the pupil size at different times during the trial. Average pupil waveforms for each condition (correct trials only). The dark green horizontal bar indicates the time cluster that shows a significant main effect of alerting ($p < 0.05$). The black-striped horizontal bar indicates the time cluster showing a significant main effect of congruency ($p < 0.05$). The gray box indicates the time window chosen for further analyses. Vertical dotted lines indicate the onset of the alerting cues and the onset and offset of the flanker stimuli. incong, incongruent; cong, congruent; catch, the small proportion of catch trials, on which the alerting cue was not followed by a flanker stimulus.

on no-alert trials (Fig. 6C; interaction, $\beta = -0.10$; 95% CI $[-0.15, -0.05]$; $t_{(26759)} = -4.27$; $p < 0.001$), supporting the hypothesis that alerting boosts the manifestation of response conflict in the brain (Asanowicz et al., 2019).

Furthermore, corroborating our hypothesis that increased TEI leads to increased response conflict, we found a statistical relationship between bilateral motor activity and theta power (Fig. 5c; Eq. 8, $\beta = -0.03$; 95% CI $[-0.06, -0.004]$; $t_{(26758)} = -2.33$; $p < 0.05$), but no relationship between the difference between contralateral and ipsilateral motor activity and theta power (Eq. 9, $\beta = 0.001$; 95% CI $[-0.03, 0.04]$; $t_{(26758)} = 0.49$; $p = 0.62$).

The effect of alerting cues on performance is partially mediated by pupil-linked arousal and EEG signature of TEI
Our theoretical account predicts that the effects of alerting cues on task performance are mediated, at least in part, by alerting effects on phasic arousal and TEI. To test this prediction, we conducted causal mixed-model mediation analyses, separately for PDR (Fig. 7a) and mean EEG over the two motor cortices (Fig. 7b). We found that there was indeed a significant average causal mediation effect (ACME) for both PDR (ACME = -0.004 ; $p < 0.001$) and mean contra/ipsi (ACME = -0.01 ; $p < 0.001$), supporting our hypothesized causal paths. However, the direct effect (DE) of alerting on RT was also strong in both analyses (PDR, DE = -0.18 ; $p < 0.001$; mean contra/ipsi,

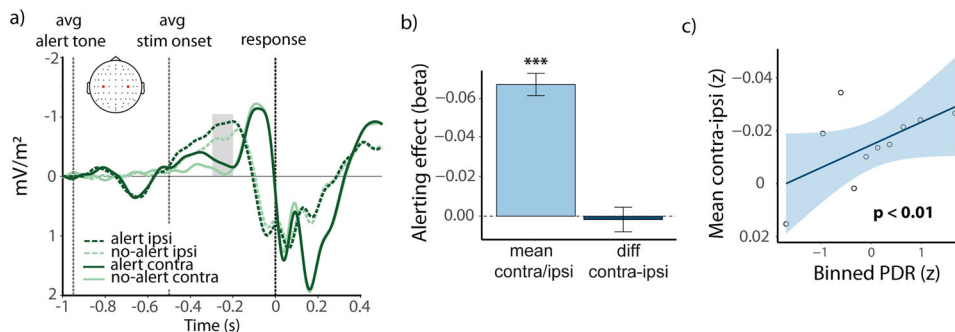


Figure 4. Alerting cues and PDR are associated with evidence-independent increase in motor cortex activity. **a**, Response-locked Laplacian–transformed EEG waveforms over the motor cortices ipsilateral and contralateral to the correct response hand (C3 and C4, red dots in the scalp image). Waveforms are averaged across congruent and incongruent trials and are based on correct trials only. Note that stimulus-evoked potentials are smeared out in these response-locked waveforms due to variability in RTs. The gray box indicates the time window chosen for subsequent analyses. **b**, Statistical effect of the alerting cues on the mean of, and difference between, EEG activity over the contralateral and ipsilateral motor cortices. The beta values shown were derived from fits of Equations 3 and 4. **c**, A scatterplot showing the association between the size of the PDR and mean EEG activity over the contralateral and ipsilateral motor cortices. The shaded area indicates 95% confidence interval. Ipsi, ipsilateral; contra, contralateral; PDR, pupil dilation response.

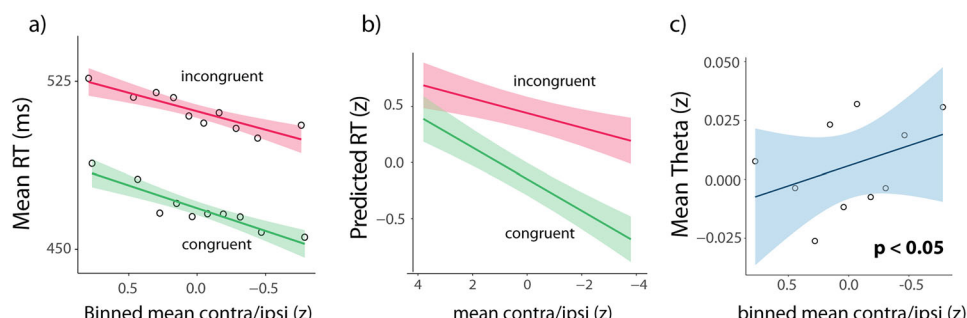


Figure 5. Higher bilateral motor cortex activity is associated with faster responses, larger congruency effects, and higher midfrontal theta power. **a**, A scatterplot linking binned bilateral motor cortex activity to mean RT. **b**, Predicted RT for a range of mean contra/ipsi values, based on the fit of Equation 6, separately for congruent and incongruent trials. The range of the mean contra/ipsi values was chosen based on the minimum and maximum values in the empirical data. **c**, A scatterplot linking binned bilateral motor cortex activity to mean theta power. Note that negative x-axis values reflect higher motor cortex activity, and thus we inverted x-axes in all panels. Shaded areas indicate 95% confidence interval.

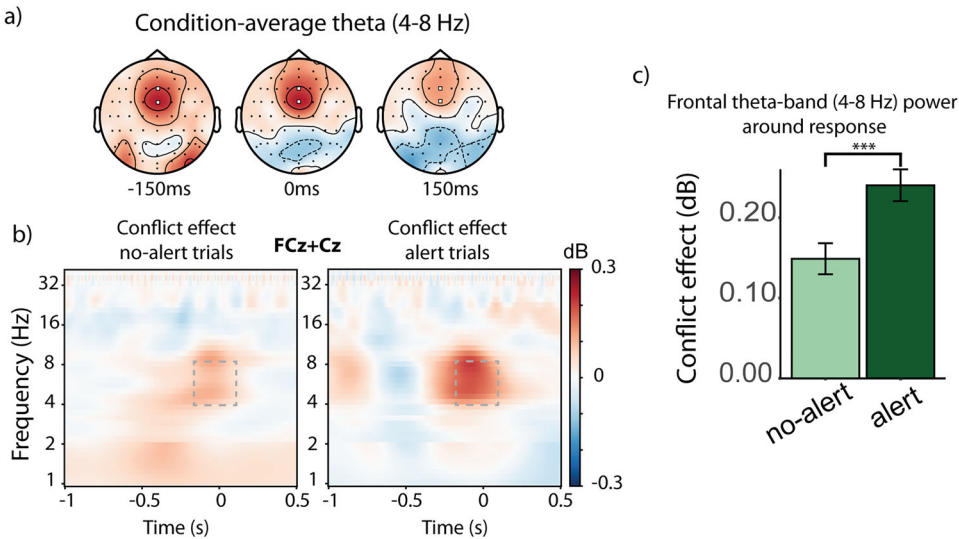


Figure 6. Midfrontal theta-band activity reveals increased response conflict in trials following an alerting cue. *a*, Response-locked scalp topographies showing scalp EEG activity in the theta band before, during, and after the response. White points denote the midfrontal (FCz and Cz) electrodes. *b*, The time–frequency plot showing the response-locked conflict effect (incongruent–congruent) for no-alert trials (left) and alert trials (right). Dotted rectangles delineate the time–frequency range, based on van Driel et al. (2015), that was used for statistical analyses. *c*, The bar plot showing that the conflict effect is larger on alert trials than on no-alert trials. dB, decibel; Hz, Hertz.

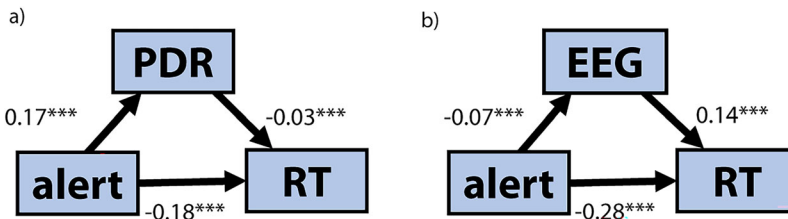


Figure 7. Alerting effects on RT are partially mediated by phasic arousal and mean activity over the contralateral and ipsilateral motor cortex. *a*, Causal mediation analysis diagram with (*a*) PDR and (*b*) mean contra/ipsi as mediators. PDR, pupil dilation response; EEG, mean contra/ipsi. *** denotes that the *p* value is smaller than 0.001.

DE = −0.28; *p* < 0.001). We discuss the implications of this latter finding in Discussion.

Drift diffusion modeling corroborates TEI account

We used DDM simulations to provide a computational proof of principle that injection of a TEI signal into the decision process can reproduce the key qualitative alerting effects on flanker-task performance by amplifying the competition between evidence accumulators. We took the following two-step approach: In Step 1, we implemented two published models of decision-making in the flanker task (Weichart et al., 2020) and fitted them to our behavioral data in the no-alert (i.e., control) condition. Then we fixed the best-fitting model parameter values. This set the stage for Step 2, in which we tested our key hypothesis: we added a TEI signal to the model and tested whether this contribution could account for the behavioral effects of alerting—that is, the difference in performance between the alert and no-alert condition. Below, we describe these steps in more detail.

Step 1

In Step 1, we selected two models from the family of SSP models (Weichart et al., 2020), which have been shown to successfully account for various aspects of flanker-task performance (White et al., 2011; Evans and Servant, 2020). Whereas in the regular DDM, the drift rate is typically considered to remain constant

over the course of a trial (aside from, in some model variants, intra-trial variability), SSP models assume that attention in the flanker task is like a spotlight of which the width is gradually reduced over the course of a trial: it is diffuse at the stimulus onset, allowing the drift rate to be influenced by the flankers, but gradually narrows in on the central target, such that the drift rate is increasingly dominated by the target. More formally, the overall decision evidence at any time point, drift rate $v(t)$, is the sum of the perceptual strength of each stimulus item weighted by the amount of attention allocated to it, which is governed by the width of the spotlight at the beginning of the trial and the rate at which the spotlight shrinks (see Materials and Methods).

SSP models, like the regular DDM, have one accumulator which can drift toward either of two fixed decision boundaries, associated with the correct and incorrect response (White et al., 2011). To examine the effect of a TEI signal on behavioral performance, the DDM must be rewritten so that it has two perfectly anticorrelated evidence accumulators that race toward the same decision threshold: If evidence for one accumulator increases, evidence for the other accumulator decreases by the same amount. In keeping with Weichart et al. (2020), we refer to this variant of the SSP diffusion model with two accumulators with crossed inhibitory inputs as the FFI model (Fig. 8).

We also considered another variant of the SSP model which was based on principles of the LCA model of two-choice RT

performance (Usher and McClelland, 2001; Weichert et al., 2020). This LCA model is similar to the FFI model, except that each accumulator in the LCA model variant passively leaks evidence over time and is inhibited by the activation of the competing accumulator through lateral inhibition (i.e., instead of FFI; Fig. 8). Previous research found that the LCA model variant, with weakly anticorrelated evidence accumulators, provided a better account of behavioral and EEG flanker-task data than the FFI with strongly anticorrelated accumulators (which features no leakage; Weichert et al., 2020).

To simulate task performance, we first determined the set of parameter values for the FFI and LCA models without TEI that best fitted the behavioral data in the no-alert condition (median RT, SD of RT, and accuracy on congruent and incongruent trials; see Materials and Methods for fitting procedure). As shown in Figure 9, the best-fitting FFI and LCA models were able to capture key features of the empirical data: the congruency effect in both RT and accuracy (Fig. 9a), skewed RT distributions with a fat tail (although both simulated distributions have fatter tails;

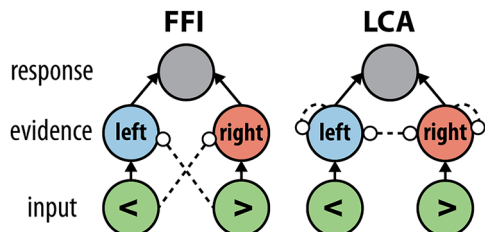


Figure 8. Schematics of the two models (Weichert et al., 2020). Solid arrows denote excitatory connections. Striped lines with circles denote inhibitory connections. FFI, feedforward inhibition; LCA, leaky-competing accumulator. Note that in the FFI model, adding TEI to one evidence unit did not affect activation of the other evidence unit.

Fig. 9b), and conditional accuracy functions that show a rapid decrease in the proportion of errors with increasing RT on incongruent trials (Fig. 9c), in line with the notion of a SSP. Given the previous success of these models in accounting for flanker-task performance and given the six and eight free parameters in these models (Table 1), it is not surprising that both the FFA model and the LCA model showed very good fits to the six data points described above. Then, importantly, we fixed the best-fitting parameter values for each model. The resulting FFA and LCA models of performance in the no-alert (i.e., control) condition provided the ideal starting point for Step 2, in which we tested our key hypothesis.

Step 2

To simulate the effects of alerting on behavior, we injected the TEI signal into each of the accumulators of the FFA and LCA models (Murphy et al., 2016). In line with the EEG modulation by alerting cues (Fig. 4a), we assumed that TEI was already maximal at the start of the decision process (corresponding to $t = 0$ in the model simulations), as characterized by a free (positive) intercept parameter. This moment corresponds to ~ 150 ms after the average stimulus-onset latency (Servant et al., 2015). Consistent with the transient nature of phasic alerting effects (Lawrence and Klein, 2013), the simulated TEI signal then diminished, as characterized by a free (negative) slope parameter. We fitted the FFA and LCA models, each with two free parameters (intercept and slope), to the behavioral data in the alert condition (six data points). We expected that if TEI causes the behavioral effects of alerting through amplification of the direct competition between the two evidence accumulators, then the LCA model but not the FFI model should be able to reproduce the empirical findings.

The best-fitting TEI parameter values (Table 1) led both models to capture the general alerting effect on RT (Fig. 10a), but as

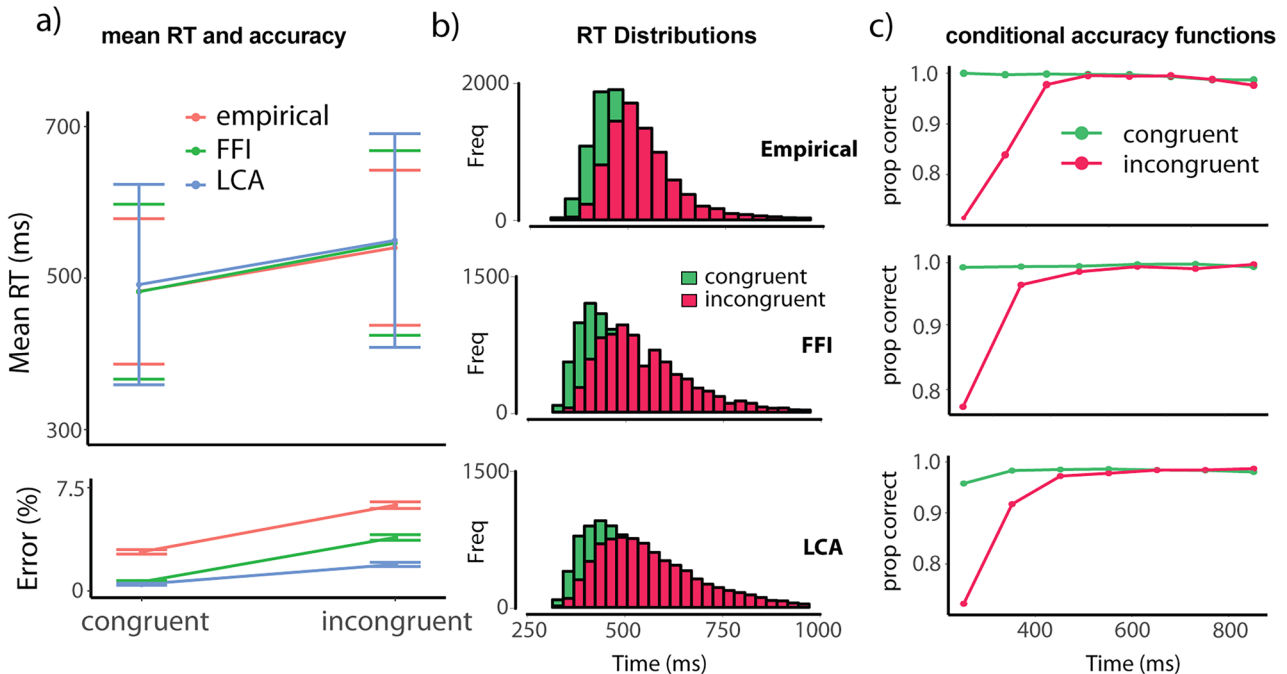


Figure 9. The FFI and LCA models provide good qualitative fits of empirical performance in the no-alert condition. **a**, Empirical and best-fitting simulated mean correct RTs (top) and error rates (bottom) show typical congruency effects. Error bars depict standard deviations. **b**, Empirical and simulated correct response-time distributions. **c**, Empirical and simulated conditional accuracy functions show the typical increase in accuracy as a function of RT. FFI, feedforward inhibition; LCA, leaky-competing accumulator; freq, frequency.

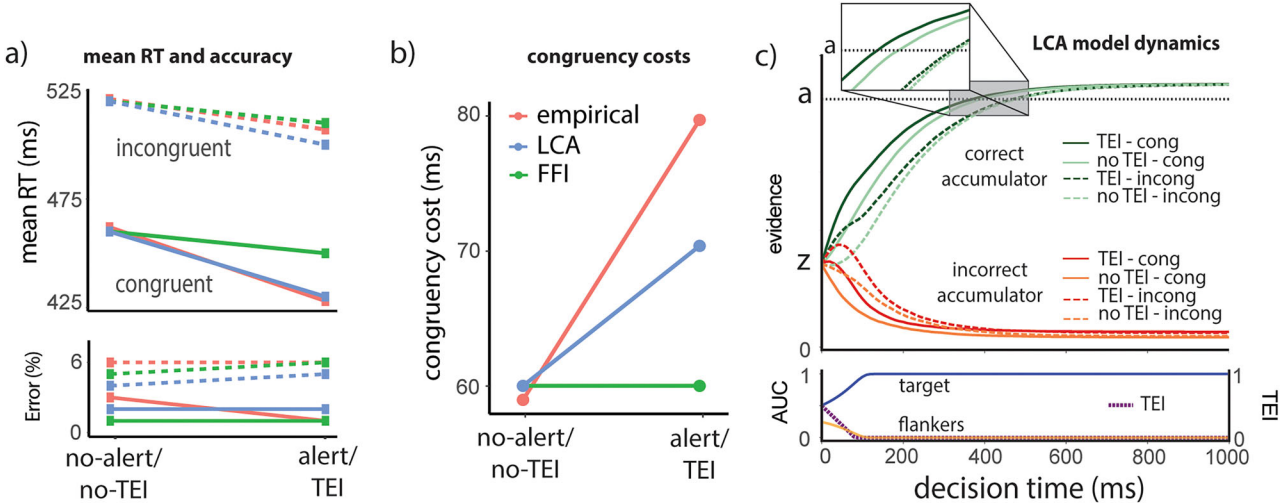


Figure 10. An LCA model with TEI can reproduce the pattern of empirical behavioral results. **a**, Empirical effects of alerting and best-fitting simulated effects of TEI on mean correct RTs (top) and error rates (bottom). **b**, Only the LCA model with TEI is able to reproduce the alert–congruency interaction. **c**, Top, The average LCA model dynamics for both accumulators, separately for each condition. The inset zooms in on the area of the plot where the correct accumulators reach the threshold (between 300 and 500 ms). Bottom, Left y-axis, the area under the curve (AUC), which corresponds to the amount of attention allocated to the target and flanker stimuli, which influences the drift rates of the correct and incorrect accumulators. Bottom, Right y-axis, the best-fitting TEI signal. Cong, congruent; incong, incongruent.

expected only the LCA model could reproduce the alert–congruency interaction (Fig. 10b). This pattern of results was robust for a range of TEI parameter values. The internal dynamics of the LCA model (Fig. 10c) confirm that TEI expedites overall RTs (i.e., the main effect of alerting) because it pushes the evidence accumulators closer to the decision threshold. The model also reproduces the main effect of congruency, because of the greater competition between the correct and incorrect accumulators on incongruent trials, especially at the start of the decision process (when the spotlight is still diffuse). This competition, through lateral inhibition, is especially pronounced in the alert condition because both accumulators receive an additional input through the TEI signal. Although the TEI signal itself is short-lived (82 ms from peak in the LCA model), its effect on the evidence accumulators slowly dissipates through passive leakage and therefore lingers after the spotlight has converged on the target and the TEI signal has returned to zero (Fig. 10c), resulting in the larger congruency effect on simulated alert trials (i.e., the alert–congruency interaction effect). The FFI model also reproduces the main effects of congruency and alerting. However, because in the FFI model there is no lateral inhibition between the two evidence accumulators (Fig. 8), the TEI inputs to the accumulators do not amplify their competition and therefore do not result in an increased congruency effect on simulated alert trials.

To complete our simulations, we considered an often-reported finding in the flanker task: congruency effects decrease when target and flankers are spaced farther apart. Schneider (2018a) examined how the alert–congruency interaction changes when the spacing between target and flankers is increased. They found that when stimuli were more widely spaced, the congruency effect was roughly halved, dropping from 79 ms for narrowly spaced flankers to 41 ms. In addition, the alert–congruency interaction was essentially abolished, dropping from 16 to 1 ms. We attempted to simulate this manipulation with our LCA model by moving the flankers away from the target (see Materials and Methods). In this setting, the simulated congruency effect dropped from 65 to 30 ms, while the alert–congruency interaction dropped from 10 to 0 ms. This nicely

replicated the qualitative pattern of results reported by Schneider. With wider stimulus spacing, the competition from the incongruent flanker was insufficient to be boosted by the TEI signal.

Discussion

Although phasic alertness generally benefits cognitive performance, it increases the impact of distracting perceptual information, resulting in impaired cognitive control (Fan et al., 2002; Callejas et al., 2005; Macleod et al., 2010; Böckler et al., 2011; Klein and Ivanoff, 2011; McConnell and Shore, 2011; Fischer et al., 2012; Weinbach and Henik, 2012; Schneider, 2018a, 2020; Kahan and Zhang, 2019). The goal of the present research was to characterize the causal pathway underlying this subtle but ubiquitous interaction between alertness and control. Our results support the hypothesized causal pathway in Figure 1, which can be summarized as follows. First, alerting cues generate a TEI signal, as indicated by a phasic increase in pupil-linked arousal, a bilateral increase in motor cortex activity, and a general speed-up of responses. Second, this TEI signal amplifies competition between evidence accumulators and thus impairs cognitive control, as indicated by behavioral and neural markers of response conflict and by simulations using an established computational model of the flanker task (Weichert et al., 2020).

If a TEI signal drives evidence accumulators closer to their common decision threshold, this will not only expedite responses but may also increase the probability of an incorrect response. That is, distracting stimulus elements (e.g., flankers) and perceptual noise may lead an incorrect accumulator to cross the decision threshold before the correct accumulator. In line with this predicted effect on the speed-accuracy trade-off, we found a minor but significant increase in error rates in the alert condition. Several perceptual decision-making studies have found a similar alerting effect on the speed-accuracy trade-off, especially studies that used relatively simple speeded tasks (with very short RTs), in which the accumulators were presumably already close to the decision threshold in the no-alert condition (Posner et al., 1973; Macleod et al., 2010; Klein, 2024). In contrast, in relatively

complex tasks, in which the accumulators tend to start at a larger distance from the decision threshold, alerting cues push the accumulators closer to the decision threshold (speeding up responses), but not sufficiently close to risk more incorrect threshold crossings (Jepma et al., 2009).

Although we propose a novel account of how phasic alertness impacts cognitive control, it is reminiscent of the facilitated response activation hypothesis (Fischer et al., 2012), according to which “...the presence of alerting signals is assumed to facilitate automatic stimulus-response translation processes for relevant and for irrelevant stimulus attributes, resulting in increased interference effects between simultaneously active response codes” (Fischer et al., 2013) and which “...is based on dual-route frameworks of response preparation and proposes amplification of both direct response activation and indirect response selection processes” (Böckler et al., 2011). That said, this hypothesis does not explicitly refer to concepts such as arousal, TEI, and evidence accumulation and lacks the computational rigor and biological detail of the present work. In support of their response activation hypothesis, Fischer and colleagues reported that they only found an alert–congruency interaction in a word flanker task when the flanker words were drawn from the same set as the target words (Fischer et al., 2012). This finding is not surprising from the perspective of our theoretical account, in which competition between evidence accumulators is an essential element. In terms of the LCA model in Figure 8, alerting cues can only impair control if the distracting stimulus feature is processed by one of the competing pathways—either because that distracting stimulus feature also serves occasionally as a target (e.g., flanker arrows) or because it has an “ideomotor-compatible” effect on that pathway. For example, laterally presented incongruent Simon-task stimuli tend to drive the incorrect processing pathway because of the way in which the visuospatial–motor circuitry in the brain is hard-wired.

Previous research has revealed the existence of decision urgency, an evidence-independent, monotonically increasing neural signal that expedites the evolving decision process by pushing it closer to a fixed decision threshold (Ditterich, 2006; Standage et al., 2011; Carland et al., 2019). There are some intriguing similarities between this monotonically growing urgency signal and the TEI signal described here. Mirroring our pupillometry and EEG findings, previous studies have found that urgency was accompanied by (1) a phasic increase in arousal (Murphy et al., 2016; Lawlor et al., 2023) and (2) a nonspecific (i.e., bimodal) increase in motor cortex activation (Thura and Cisek, 2016); (3) both urgency and phasic alerting (and hence TEI) have been associated with an increase in response vigor (Ulrich and Matthes, 1996; Thura and Cisek, 2014, 2016), and (4) both urgency and TEI have the purpose of speeding up RTs—either in the service of maximizing the reward rate (urgency; Carland et al., 2019) or to mobilize the system for rapid action in response to arousing events (TEI). These similarities suggest a close relationship between the computational and physiological bases of urgency and TEI.

Our cue-target interval of 500 ms, although commonly used to study phasic alertness, was long enough to allow a bit of time for (voluntary) temporal preparation (Hackley, 2009; Nobre and van Ede, 2018). This raises the question of whether some of the differences in results between the alert and no-alert conditions reflect in part an effect of temporal preparation instead of phasic arousal. Importantly, our mediation analyses revealed that the observed alerting effect on RT was significantly mediated by the PDR and by bilateral motor cortex activity,

consistent with our proposal that the effects of alerting cues on task performance are mediated by phasic arousal and TEI. However, the mediation was partial, not full; both mediation analyses also revealed a significant DE of alerting on RT. Although we discouraged voluntary temporal preparation, using catch trials to weaken the temporal contingency between alerting cues and flanker stimuli, we cannot exclude the possibility that these DEs were caused by temporal preparation. Indeed, preliminary evidence suggests that temporal preparation has similar effects on overall response speed and cognitive control as phasic alertness (Correa et al., 2010; Weinbach and Henik, 2013). Interestingly, recent evidence suggests that temporal preparation is accompanied by a gradual increase in the pupil size and urgency (Lawlor et al., 2023). This raises the intriguing possibility that alerting cues can cause not only a rapid increase in arousal and TEI, as reported here, but also a well-timed, relatively slow increase in arousal and urgency over the course of a predictable cue-target interval.

The largest challenge for any account of the alert–congruency interaction is that this interaction is not found for all conflict tasks. It is found in variants of the arrow flanker task (MacLeod et al., 2010; Schneider, 2018b), the Simon task (Böckler et al., 2011; Klein and Ivanoff, 2011), global/local task (Weinbach and Henik, 2014), and spatial Stroop task (i.e., classify the spatial meaning of a stimulus presented at an irrelevant position; Schneider, 2020). By far, the most prominent example of a task that consistently fails to show the alert–congruency interaction is the manual color-word Stroop task (Weinbach and Henik, 2012; Schneider, 2019a). Most of the evidence suggests that the interaction only occurs in tasks requiring spatial attention and spatial information processing, and therefore not in tasks such as the Stroop task in which the relevant and irrelevant stimulus dimensions are spatially integrated (Schneider, 2019a, 2020). However, why this might be the case is still poorly understood.

Weinbach and Henik (2012) proposed the attractive hypothesis that alerting causes a more diffuse focus of attention, resulting in more processing of spatially separate distracting information (e.g., flankers) and a corresponding increase in the flanker congruency effect. However, this hypothesis and two closely related accounts involving spatial attention (Nieuwenhuis and de Kleijn, 2013; Schneider, 2018a) have not been supported in recent tests (Schneider, 2018a, 2019b; Seibold, 2018). Alternatively, the distracting stimulus features in spatial conflict tasks (e.g., arrow flankers or the stimulus location in the Simon task and spatial Stroop task) tend to have directional associations (e.g., left/right or up/down) that can be mapped onto the spatial codes used in responding (Kornblum et al., 1999; Fischer et al., 2012; Kahan and Zhang, 2019). Perhaps this is a necessary requirement for finding an alert–congruency interaction. That is, an alerting cue may not boost activation along the incorrect pathway when the distracting stimulus feature (e.g., a color word) does not have directional associations with the response set (e.g., left and right response keys), as is the case in the manual color-word Stroop task (Schneider, 2019a). Future studies should examine whether in tasks without directional associations alerting cues elicit a nonspecific increase in motor cortex activation, our electrophysiological index of TEI.

Data Availability

The datasets generated and analyzed during the current study, Python scripts used for the model simulations, and the R script used for fitting the linear models are available on OSF: <https://osf.io/vhq76/>.

References

- Anasowicz D, Wołoszyn K, Panek B, Wronka E (2019) On the locus of the effect of alerting on response conflict: an event-related EEG study with a speed-accuracy tradeoff manipulation. *Biol Psychol* 145:62–75.
- Böckler A, Alpay G, Stürmer B (2011) Accessory stimuli affect the emergence of conflict, not conflict control. *Exp Psychol* 58:102–109.
- Bogacz R, Cohen JD (2004) Parameterization of connectionist models. *Behav Res Methods Instrum Comput* 36:732–741.
- Brown SBRE, Tona K-D, van Noorden MS, Giltay EJ, van der Wee NJA, Nieuwenhuis S (2015) Noradrenergic and cholinergic effects on speed and sensitivity measures of phasic alerting. *Behav Neurosci* 129:42–49.
- Callejas A, Lupiáñez J, Funes MJ, Tudela P (2005) Modulations among the alerting, orienting and executive control networks. *Exp Brain Res* 167: 27–37.
- Carland MA, Thura D, Cisek P (2019) The urge to decide and act: implications for brain function and dysfunction. *Neuroscientist* 25:491–511.
- Cohen MX, Cavanagh JF (2011) Single-trial regression elucidates the role of prefrontal theta oscillations in response conflict. *Front Psychol* 2:30.
- Correa A, Triviño M, Pérez-Dueñas C, Acosta A, Lupiáñez J (2010) Temporal preparation, response inhibition and impulsivity. *Brain Cogn* 73:222–228.
- de Gee JW, Colizoli O, Kloosterman NA, Knapen T, Nieuwenhuis S, Donner TH (2017) Dynamic modulation of decision biases by brainstem arousal systems. *eLife* 6:e23232.
- Dietze N, Poth CH (2024) Phasic alerting in visual search tasks. *Atten Percept Psychophys* 86:707–716.
- Ditterich J (2006) Evidence for time-variant decision making. *Eur J Neurosci* 24:3628–3641.
- Evans NJ, Servant M (2020) A comparison of conflict diffusion models in the flanker task through pseudolikelihood Bayes factors. *Psychol Rev* 127: 114–135.
- Fan J, McCandliss BD, Sommer T, Raz A, Posner MI (2002) Testing the efficiency and independence of attentional networks. *J Cogn Neurosci* 14: 340–347.
- Fischer R, Plessow F, Kiesel A (2012) The effects of alerting signals in action control: activation of S-R associations or inhibition of executive control processes? *Psychol Res* 76:317–328.
- Fischer R, Plessow F, Kiesel A (2013) The effects of alerting signals in masked priming. *Front Psychol* 4:448.
- Grant SJ, Aston-Jones G, Redmond DE Jr (1988) Responses of primate locus coeruleus neurons to simple and complex sensory stimuli. *Brain Res Bull* 21:401–410.
- Gratton G, Coles MGH, Sirevaag EJ, Erikson CW, Donchin E (1988) Pre- and poststimulus activation of response channels: a psychophysiological analysis. *J Exp Psychol Hum Percept Perform* 14:331–344.
- Gross MP, Dobbins IG (2021) Pupil dilation during memory encoding reflects time pressure rather than depth of processing. *J Exp Psychol Learn Mem Cogn* 47:264–545.
- Hackley SA (2009) The speeding of voluntary reaction by a warning signal. *Psychophysiology* 46:225–233.
- Jankovic N, Di Lollo V, Spalek TM (2022) Alerting effects occur in simple-but not in compound-visual search tasks. *J Exp Psychol Hum Percept Perform* 48:901–912.
- Jepma M, Wagenmakers E-J, Band GPH, Nieuwenhuis S (2009) The effects of accessory stimuli on information processing: evidence from electrophysiology and a diffusion model analysis. *J Cogn Neurosci* 21:847–864.
- Joshi S, Gold JI (2020) Pupil size as a window on neural substrates of cognition. *Trends Cogn Sci* 6:466–480.
- Joshi S, Li Y, Kalwani RM, Gold JI (2016) Relationships between pupil diameter and neuronal activity in the locus coeruleus, colliculi, and cingulate cortex. *Neuron* 89:221–234.
- Kahan TA, Zhang H (2019) Ready to be distracted: further evidence that the alerting-congruity interaction requires stimulus-response directional associations. *Vis Cogn* 27:760–767.
- Klein RM (2024) Assessing the predictions from Posner's theory of phasic alertness using data from Los and Schut (2008). *Mem Cogn* 52:1–6.
- Klein RM, Ivanoff J (2011) The components of visual attention and the ubiquitous Simon effect. *Acta Psychol* 136:225–234.
- Kornblum S, Stevens GT, Whipple A, Requin J (1999) The effects of irrelevant stimuli: 1. The time course of stimulus-stimulus and stimulus-response consistency effects with Stroop-like stimuli, Simon-like tasks, and their factorial combinations. *J Exp Psychol Hum Percept Perform* 25: 688–714.
- Kret ME, Sjak-Shie EE (2019) Preprocessing pupil size data: guidelines and code. *Behav Res Methods* 51:1336–1342.
- Kusnir F, Chica AB, Mitsumasu MA, Bartolomeo P (2011) Phasic auditory alerting improves visual conscious perception. *Conscious Cogn* 20: 1201–1210.
- Lawlor J, Zagala A, Jamali S, Boubenec Y (2023) Pupillary dynamics reflect the impact of temporal expectation on detection strategy. *iScience* 26:106000.
- Lawrence MA, Klein RM (2013) Isolating exogenous and endogenous modes of temporal attention. *J Exp Psychol Gen* 142:560–572.
- Macleod JW, Lawrence MA, McConnell MM, Eskes GA, Klein RM, Shore DI (2010) Appraising the ANT: psychometric and theoretical considerations of the Attention Network Test. *Neuropsychology* 24:637–651.
- Mathôt S (2018) Pupillometry: psychology, physiology, and function. *J Cogn* 1:16.
- Mathôt S, Vilotijević A (2022) Methods in cognitive pupillometry: design, preprocessing, and statistical analysis. *Behav Res Methods* 55: 3055–3077.
- McConnell MM, Shore DI (2011) Mixing measures: testing an assumption of the Attention Network Test. *Atten Percept Psychophys* 73:1096–1107.
- Murphy PR, Boonstra E, Nieuwenhuis S (2016) Global gain modulation generates time-dependent urgency during perceptual choice in humans. *Nat Commun* 7:13526.
- Nieuwenhuis S, de Kleijn R (2013) The impact of alertness on cognitive control. *J Exp Psychol Hum Percept Perform* 39:1797–1801.
- Nobre AC, van Ede F (2018) Anticipated moments: temporal structure in attention. *Nat Rev Neurosci* 19:34–48.
- Petersen SE, Posner MI (2012) The attention system of the human brain: 20 years after. *Annu Rev Neurosci* 35:73–89.
- Petersen A, Petersen AH, Bundesen C, Vangkilde S, Habekost T (2017) The effect of phasic auditory alerting on visual perception. *Cognition* 165:73–81.
- Posner MI, Klein R, Summers J, Buggie S (1973) On the selection of signals. *Mem Cogn* 1:2–12.
- Posner MI (2008) Measuring alertness. *Ann N Y Acad Sci* 1129:193–199.
- Poth CH (2021) Urgency forces stimulus-driven action by overcoming cognitive control. *eLife* 8:1196–1204.
- Schneider DW (2018a) Alertness and cognitive control: toward a spatial grouping hypothesis. *Atten Percept Psychophys* 80:913–928.
- Schneider DW (2018b) Alertness and cognitive control: testing the early onset hypothesis. *J Exp Psychol Hum Percept Perform* 44:756–766.
- Schneider DW (2019a) Alertness and cognitive control: is there a spatial attention constraint? *Atten Percept Psychophys* 81:119–136.
- Schneider DW (2019b) Alertness and cognitive control: testing the spatial grouping hypothesis. *Atten Percept Psychophys* 81:1913–1925.
- Schneider DW (2020) Alertness and cognitive control: interactions in the spatial Stroop task. *Atten Percept Psychophys* 82:2257–2270.
- Seibold VC (2018) Do alerting signals increase the size of the attentional focus? *Atten Percept Psychophys* 80:402–425.
- Servant M, White C, Montagnini A, Burle B (2015) Using covert response activation to test latent assumptions of formal decision-making models in humans. *J Neurosci* 35:10371–10385.
- Singh GS, Acerbi L (2024) PyBADS: fast and robust black-box optimization in Python. *J Open Source Softw* 9:5694.
- Standage D, You H, Wang D-H, Dorris MC (2011) Gain modulation by an urgency signal controls the speed-accuracy trade-off in a network model of a cortical decision circuit. *Front Comput Neurosci* 5:7.
- Steinemann NA, O'Connell RG, Kelly SP (2018) Decisions are expedited through multiple neural adjustments spanning the sensorimotor hierarchy. *Nat Commun* 9:3627.
- Thura D, Cisek P (2014) Deliberation and commitment in the premotor and primary motor cortex during dynamic decision making. *Neuron* 81:1401–1416.
- Thura D, Cisek P (2016) Modulation of premotor and primary motor cortical activity during volitional adjustments of speed-accuracy trade-offs. *J Neurosci* 36:938–956.
- Tingley D, Yamamoto T, Hirose K, Keele L, Imai K (2014) Mediation: R package for causal mediation analysis. *J Stat Softw* 59:1–38.
- Tona K-D, Murphy PR, Brown SBRE, Nieuwenhuis S (2016) The accessory stimulus effect is mediated by phasic arousal: a pupillometry study. *Psychophysiology* 53:1108–1113.
- Ulrich R, Matthes S (1996) Does immediate arousal enhance response force in simple reaction time? *Q J Exp Psychol A* 49:972–990.

- Usher M, McClelland JL (2001) The time course of perceptual choice: the leaky, competing accumulator model. *Psychol Rev* 108:550–592.
- van der Wel P, van Steenbergen H (2018) Pupil dilation as an index of effort in cognitive control tasks: a review. *Psychon Bull Rev* 25:2005–2015.
- van Driel J, Swart JC, Egner T, Ridderinkhof KR, Cohen MX (2015) (No) time for control: frontal theta dynamics reveal the cost of temporally guided conflict anticipation. *Cogn Affect Behav Neurosci* 15:787–807.
- Vidal F, Burle B, Spieser L, Carbonnell L, Meckler C, Casini L, Hasbroucq T (2015) Linking EEG signals, brain functions and mental operations: advantages of the Laplacian transformation. *Int J Psychophysiol* 97: 221–232.
- Weichart ER, Turner BM, Sederberg PB (2020) A model of dynamic, within-trial conflict resolution for decision making. *Psychol Rev* 127:749–777.
- Weinbach N, Henik A (2012) The relationship between alertness and executive control. *J Exp Psychol Hum Percept Perform* 38:1530–1540.
- Weinbach N, Henik A (2013) The interaction between alerting and executive control: dissociating phasic arousal and temporal expectancy. *Atten Percept Psychophys* 75:1374–1381.
- Weinbach N, Henik A (2014) Alerting enhances attentional bias for salient stimuli: evidence from a global/local processing task. *Cognition* 133:414–419.
- White CN, Ratcliff R, Sterns JJ (2011) Diffusion models of the flanker task: discrete versus gradual attentional selection. *Cogn Psychol* 63:210–238.